文章编号：1001－9014(2018)06－0688－05

DOI:10.11972/j.issn.1001－9014.2018.06.009

An approach to determine small-signal model parameters for InP HBT up to 110 GHz

ZHANG Ao, ZHANG Yi-Xin, WANG Bo-Ran, GAO Jian-Jun*

(School of Information Science Technology, East China Normal University, Shanghai 200241, China)

Abstract: An approach for determination of small-signal equivalent circuit model elements for InP HBT is presented in this paper. The skin effect of the feedlines is taken into account in the proposed model. This method combines the analytical approach and empirical optimization procedure. The intrinsic elements determined by a conventional analytical parameter transformation technique are described as function of extrinsic resistances. An excellent fit between measured and simulated S-parameters in the frequency range of 2～110 GHz is obtained for InP HBT.

Key words: equivalent circuits, heterojunction bipolar transistor(HBT), device modeling

PACS: 85.30.De

110 GHz 铟磷异质结双极晶体管小信号模型参数提取方法

张 傲, 张译心, 王博冉, 高建军*

(华东师范大学 信息科学技术学院,上海 200241)

摘要:介绍了一种可以用于频率高达110 GHz的InP基HBT小信号模型模型参数提取方法,并且在所提出的模型中考虑了基极馈线的趋肤效应.该方法将直接提取和优化技术相结合,将本征参数描述为寄生电阻的系列函数进行后续优化.实验结果表明在2～110 GHz频率范围内S参数吻合很好.

关 键 词:等效电路模型;异质结双极晶体管;器件建模

中图分类号:TN386.6 **文献标识码**:A

Introduction

The heterojunction bipolar transistor (HBT) is a type of bipolar junction transistor which uses differing semiconductor materials for the emitter and base regions, creating a heterojunction. The advantages of HBT's in high-speed applications result from two features: their structure and their superior carrier transport properties.

In the high-frequency characterization of microwave transistors, the non-linear models used in the design of HBT integrated circuits are based on the π-type equivalent circuit model and the small signal linear models are based on the T-type structure[1-2]. Compared with the π-type equivalent circuit model, T-type equivalent circuit model is appealing because all the model parameters can be directly tied to the physics of the device, while HBT π-type model is similar with conventional FET small signal equivalent circuit model to help researchers easier to modeling and extracting the parameters. However, studies show that π-type model and T-type model can both be made exactly equivalent if the frequency dependences of model parameters are correctly modeled, which is why the two models can coexist[3-6]. For historical reasons dating back to silicon based bipolar transistor development, the Gummel Poon model is used by most bipolar circuit designers and as a standard nonlinear model in integrated circuit simulators, and the Gummel Poon model reduces to the hybrid π-topology under small signal conditions. This requires compact large-signal models to be formulated in π-topology.

The objective of this paper is to establish an π-topology equivalent-circuit model for InP HBT over a wide frequency range up to millimeter-wave frequencies. In contrast with previous publications, this method has the advantages as follows.

1) An improved model of the feedline incorporating skin and proximity effects is adopted.

2) The parameter extraction method is based on the combination of the analytical approach and empirical op-

Received date: 2018-03-30, **revised date**: 2018-08-24 **收稿日期**:2018-03-30, **修回日期**:2018-08-24

Foundation items: Supported by National Natural Science Foundation of China (61774058)

Biography: ZHANG Ao (1995-), female, Nanjing, China, master. Research area involves microwave device modeling. E-mail: zhangao78@qq.com

* **Corresponding author**: E-mail: jjgao@ee.ecnu.edu.cn

timization procedure. The intrinsic elements are described as function of extrinsic resistances.

3) The model has been verified up to 110 GHz with very good accuracy.

In the following sections, we introduce the used small signal topologies, the modeling procedure. Finally, we present the parameter extraction and the comparison of modeled and measured data.

1 Equivalent circuit model

In on-wafer measurements, a GSG pad structure for probe touching is needed. Figure 1 shows a typical HBTs test structure pattern which consists of one signal line and two ground lines and it consists of the input signal, the output signal and ground to equivalent circuit model with three capacitances. Access to the devices is normally made through coplanar waveguide probes. When microwave frequency measurements are made, signals are brought to the HBT by the transmission lines. The parasitic effects due to the test geometry will have significant effects on the measured results.

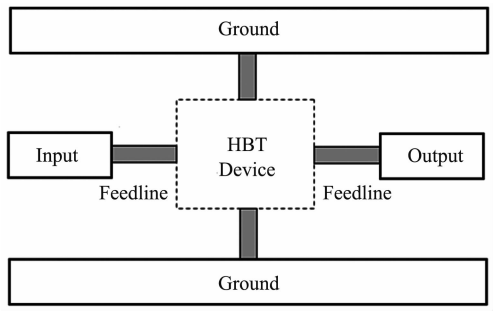

Fig. 1　HBT device test structure
图 1　HBT 器件测试结构

The skin effect is a well-known physical phenomenon, which results in a vertically and laterally nonuniform current flow in a rectangular conductor. But for systems operating at millimeter wave frequency, the skin effect of the feedlines must be considered, it has been extensively studied by many researchers, but it′s not been taken into account in modeling of HBTs. Therefore, the model of the extrinsic part should be improved.

Figure 2 shows the proposed equivalent circuit model of extrinsic part, where $C_{\rm pb}$, $C_{\rm pc}$ and $C_{\rm pbc}$ represent the base, collector and isolation between base and collector pad capacitances. $L_{\rm b}$, $L_{\rm c}$ and $L_{\rm e}$ represent the inductances of the base, collector, and emitter device-connection, respectively. Compared with conventional model, an *RL* ladder network comprising frequency-independent R_k and L_k elements are used to model the skin effect of base feedline. It must be noted that, based on our experimental results, skin effects of the collector and emitter feedlines can be neglected. Note the pad capacitance $C_{\rm pb}$ and $C_{\rm pc}$ are placed inside of the feedline inductances.

Figure 3 shows the intrinsic network. It can be found that HBT π-type model is similar with conventional FET small signal equivalent circuit model. The input impedance is $Z_\pi = R_\pi + j\omega C_\pi$, which consists of the base-emitter resistance R_π and capacitance C_π. Feedback network consists of R_μ and C_μ. *Y* parameters can be expressed as:

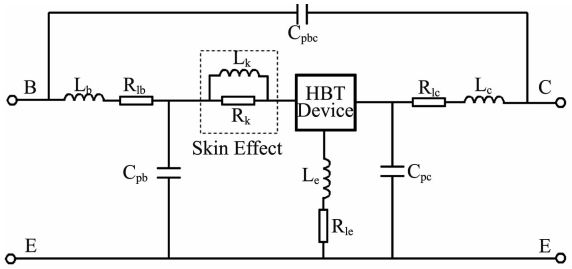

Fig. 2　Proposed equivalent circuit model of extrinsic part
图 2　提出寄生部分的等效电路模型

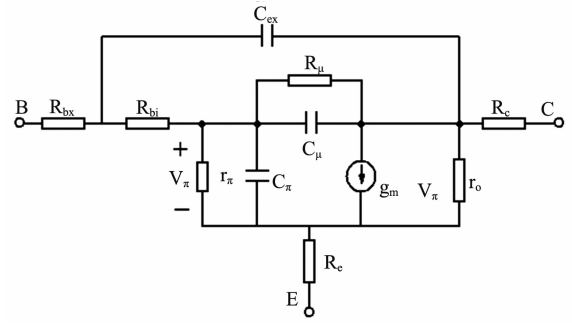

Fig. 3　π-type intrinsic model for HBT
图 3　π 型 HBT 器件本征电路模型

$$Y_{11} = \frac{1 + j\omega r_x(C_\pi + C_\mu)}{(r_\pi + R_{bi}) + j\omega R_{bi} r_\pi (C_\pi + C_\mu)} + j\omega C_{ex} \quad , \quad (1)$$

$$Y_{12} = \frac{j\omega r_\pi C_\mu}{(r_\pi + R_{bi}) + j\omega R_{bi} r_\pi (C_\pi + C_\mu)} + j\omega C_{ex} \quad , \quad (2)$$

$$Y_{21} = \frac{g_m r_\pi e^{j\omega\tau_\pi} - j\omega r_\pi C_\mu}{(r_\pi + R_{bi}) + j\omega R_{bi} r_\pi (C_\pi + C_\mu)} + j\omega C_{ex} \quad , \quad (3)$$

$$Y_{22} = \frac{r_\pi / r_o + j\omega r_\pi C_\mu + r_\pi R_{bi}\Delta Y}{(r_\pi + R_{bi}) + j\omega R_{bi} r_\pi (C_\pi + C_\mu)} + j\omega C_{ex} \quad , \quad (4)$$

where g_m is the DC trans-conductance.

$$g_m = g_{m0}\exp(-j\omega\tau_\pi)$$

2 Parameter extraction

The extraction of the parasitic elements and the intrinsic model parameters can be carried out using the procedure as follows:

1) The extrinsic capacitances are obtained directly from the S-parameters of the open test structure.

$$C_{\rm pb} = \frac{1}{\omega}{\rm Im}(Y_{11} + Y_{12}) \quad , \quad (5)$$

$$C_{\rm pc} = \frac{1}{\omega}{\rm Im}(Y_{22} + Y_{12}) \quad , \quad (6)$$

$$C_{\mathrm{pbc}} = -\frac{1}{\omega}\mathrm{Im}(Y_{12}) = -\frac{1}{\omega}\mathrm{Im}(Y_{21}) \quad . \quad (7)$$

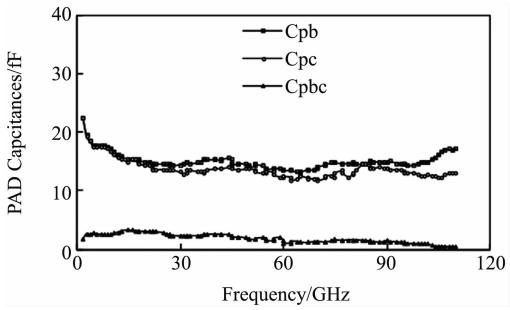

Fig. 4 Extracted PAD capacitances
图4 提取的寄生PAD电容数值

Figure 4 shows the extracted parasitic PAD capacitanc versus frequency. We can see that the input and output port extrinsic capacitances are about 14 fF, while the coupling capacitance between the ports is 2 fF.

2) The extrinsic inductances are obtained directly from the S-parameters of the short test structure.

$$L_{\mathrm{e}} = \frac{1}{\omega}\mathrm{Im}(Z_{12}) = \frac{1}{\omega}\mathrm{Im}(Z_{21}) \quad , \quad (8)$$

$$L_{\mathrm{b}} = \frac{1}{\omega}\mathrm{Im}(Z_{11} - Z_{12}) \quad , \quad (9)$$

$$L_{\mathrm{c}} = \frac{1}{\omega}\mathrm{Im}(Z_{22} - Z_{21}) \quad . \quad (10)$$

Figure 5 shows the frequency dependence of the extrinsic inductances, constant values are observed from 2 GHz to 110 GHz with the deviations from the mean values being less than 5%. That means the feedline inductances are frequency independent, of course also bias independent. Figure 6 shows the extracted base feedline resistance R_{lb} versus frequency, it is clear that R_{lb} increases with increase of frequency. As well known, skin effect is a tendency for alternating current to flow mostly near the outer surface of a solid electrical conductor, such as metal wire, at frequencies above the audio range. The effect becomes more and more apparent as the frequency increases. An *RL* ladder network comprising frequency-independent R_k and L_k elements are used to model the skin effect of base feedline. From Fig. 6, the based feedline model parameters can be determined directly: $R_{\mathrm{lbo}} = 0.1\ \Omega$, $L_k = 4$ pH.

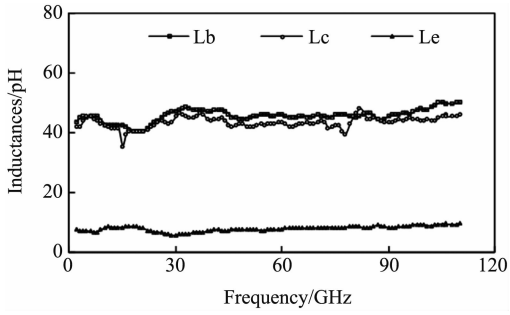

Fig. 5 Extracted extrinsic inductances
图5 提取的寄生电感数值

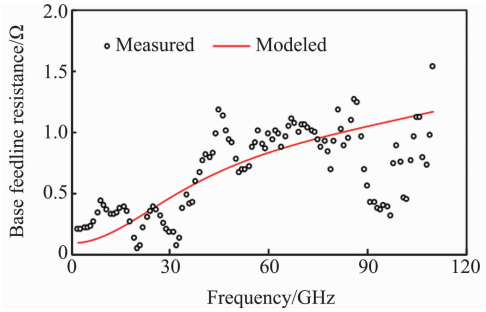

Fig. 6 Extracted feedline rersistance R_{lb}
图6 提取的馈线电阻 R_{lb}

3) Set the initial value of the extrinsic resistances R_{bx}, R_{c} and R_{e}.

4) Calculation of the intrinsic elements, which can be expressed as the functions of the extrinsic resistances as well as frequency.

$$R_{\pi} = f_1(R_{\mathrm{bx}}, R_{\mathrm{c}}, R_{\mathrm{e}}) \quad , \quad (11)$$

$$C_{\pi} = f_2(R_{\mathrm{bx}}, R_{\mathrm{c}}, R_{\mathrm{e}}) \quad , \quad (12)$$

$$C_{\mathrm{ex}} = f_3(R_{\mathrm{bx}}, R_{\mathrm{c}}, R_{\mathrm{e}}) \quad , \quad (13)$$

$$C_{\mathrm{bc}} = f_4(R_{\mathrm{bx}}, R_{\mathrm{c}}, R_{\mathrm{e}}) \quad , \quad (14)$$

$$g_{\mathrm{m}} = f_5(R_{\mathrm{bx}}, R_{\mathrm{c}}, R_{\mathrm{e}}) \quad , \quad (15)$$

$$\tau = f_6(R_{\mathrm{bx}}, R_{\mathrm{c}}, R_{\mathrm{e}}) \quad , \quad (16)$$

$$R_{\mathrm{bi}} = f_7(R_{\mathrm{bx}}, R_{\mathrm{c}}, R_{\mathrm{e}}) \quad . \quad (17)$$

For convenience, the function f_k can be expressed as follows:

$$f_k = f_k(\omega_i, R_{\mathrm{ext}})(k = 0,1\cdots\cdots 7) \quad , \quad (18)$$

where R_{ext} represent the extrinsic resistances, ω_i is the angular frequency.

Setup error criteria as follows:

$$\varepsilon(Z_{\mathrm{ext}}) = \frac{1}{N-1}\sum_{i=0}^{N-1}\left|f_k(\omega_i, R_{\mathrm{ext}}) - \overline{\sum_{i=0}^{N-1} f_k(\omega_i, R_{\mathrm{ext}})}\right|^2 \quad (p,q = 1,2) \quad , \quad (19)$$

$$\varepsilon_2(Z_{\mathrm{ext}}) = \sum\sum\sum W_{pq}\left|S_{pq}^{c}(\omega_i, R_{\mathrm{ext}}) - S_{pq}^{m}(\omega_i)\right|^2 \quad (p,q = 1,2) \quad , \quad (20)$$

where $S_{pq}^{c}(\omega_i, Z_{\mathrm{ext}})$ represents the calculated S parameters, $S_{pq}^{m}(\omega_i)$ represents the measured S parameters.

5) If error criteria are small enough, the iterative process will be over.

The extracting process is illustrated as Fig. 6, it can be found that a parameter-extraction approach for the HBT, which combines the analytical approach and empirical optimization procedure is adopted.

3 Results and discussion

The InP HBTs used in this work were grown by gas-source molecular beam epitaxy on semi-insulating InP substrates supplied by a commercial vendor. Be and Si are used for p- and n-type dopants, respectively. The detailed layer structure of the InP/InGaAsInP DHBT is shown in Table I[7-8].

The S-parameter measurements for 5 μm × 5 μm InP/InGaAs DHBTs and verification were made up to 110 GHz using HP8510XF network analyzer, with DC bias was supplied by Agilent HP4156. All measurements

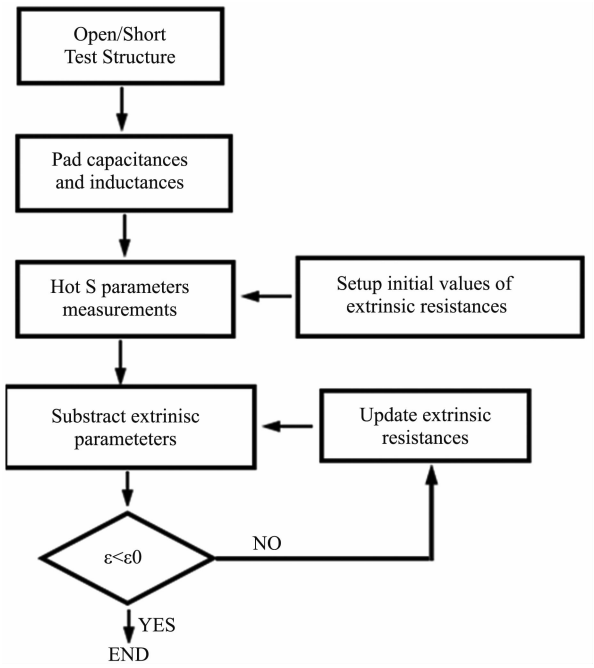

Fig. 7　Flow chart of the algorithm
图 7　算法框图

Table 1　Epitaxial structure of InP/InGaAs/InP DHBT
表 1　InP/InGaAs/InP DHBT 的外延结构

Layers	Thickness/nm	Doping/cm^{-3}
InGaAs CAP	100	$n^+ = 2\times10^{19}$
InP CAP	60	$n^+ = 2\times10^{19}$
InP Emitter	90	$n = 3\times10^{17}$
InGaAs Base	47	$p^+ = 2\times10^{19}$
InGaAs Collector	40	$n^- = 5\times10^{15}$
InGaAs Collector	10	$p = 2\times10^{18}$
InP Collector	10	$n = 1\times10^{18}$
InP Collector	290	$n^- = 5\times10^{15}$
InP Subcollector	8	$n^+ = 5\times10^{18}$
InGaAs Subcollector	450	$n^+ = 5\times10^{18}$
S. I. Substrate		

were carried out on wafer using Cascade Microtech's Air-Coplanar Probes ACP50-GSG-100. Details of the device structure and fabrication technique have been described elsewhere[7-8]. The values of the model elements are as following: $R_{bx} = 4\ \Omega$, $R_c = 16\ \Omega$, $R_e = 1.8\ \Omega$, $C_{ex} = 41$ fF, $R_{bi} = 130\ \Omega$, $R_x = 220\ \Omega$, $C_\pi = 0.28$ pF. $g_m = 188$ mS.

In Fig. 7, the modeled S parameters for short test structure (as seen in Fig. 2) are compared with measured data for the InP HBT under the bias conditions ($I_b = 100\ \mu$A and $V_{CE} = 1.5$ A). A good agreement can be observed. The above computed data are also compared with the conventional model. It shows that the proposed model is more accurate than the conventional one.

Figure 8 shows the comparison of modeled and measured S parameters for the HBTs in the frequency range of 2 ~ 110 GHz, good agreement is obtained to verify the validity of the proposed method.

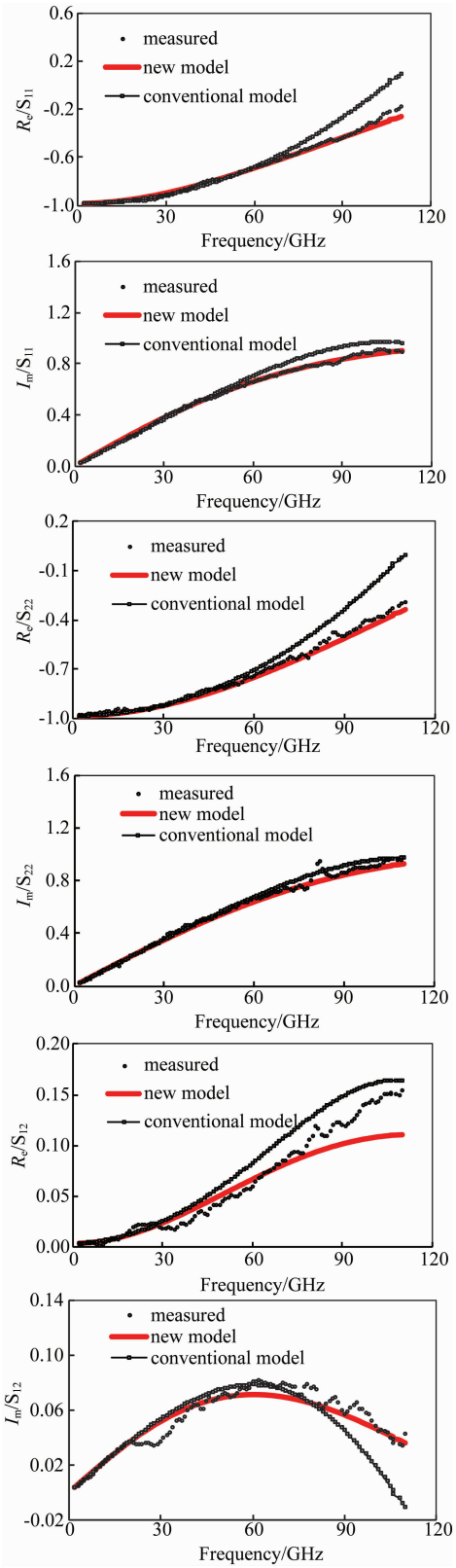

Fig. 8　Comparison of modeled and measured S parameters for the short test structure
图 8　短路测试结构 S 参数的模拟和对比曲线

4　Conclusion

An approach for determination of small-signal equiv-

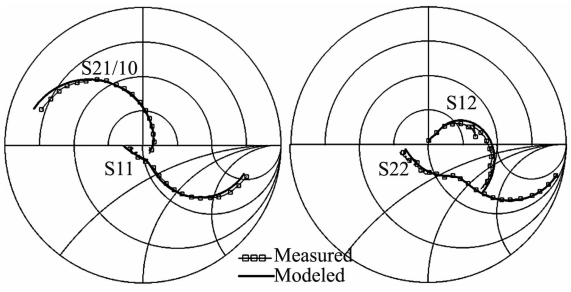

Fig. 9 Comparison of modeled and measured S parameters for the HBTs in the frequency range of 2 ~ 110 GHz, Bias: I_b = 100 μA and V_{CE} = 1.5 V

图 9 2 ~ 110 GHz 频率范围内 HBT 器件 S 参数的模拟和对比曲线,偏置:I_b = 100 μA 和 V_{CE} = 1.5 V

alent circuit model elements for InP HBT is presented in this paper. The intrinsic elements determined by a conventional analytical parameter transformation technique are described as function of extrinsic resistances. An excellent fit between measured and simulated S-parameters in the frequency range of 2 ~ 110 GHz is obtained for InP HBT.

References

[1] Gao J. *Heterojunction bipolar transistor for circuit design—Microwave modeling and parameter extraction*[M]. Singapore: Wiley, 2015.

[2] McMacken J, Nedeljkovic S, Gering J, *et al.* HBT modeling [J]. *IEEE Microwave Magazine*, 2008, **9**(2): 48 - 71.

[3] Johansen T K, Leblanc R, Poulain J, *et al.* Direct extraction of InP/GaAsSb/InP DHBT equivalent-circuit elements from S-parameters measured at cut-off and normal bias conditions[J]. *IEEE Trans. Microw. Theory Techn.*, 2016, **64**(1):115 - 123.

[4] Gao J, Li X, Wang H., *et al.* An improved analytical method for determination of small signal equivalent circuit model parameters for InP/InGaAs HBTs[J]. *IEE Proceedings - Circuit, Device and System*, 2005, **152**(6): 661 - 666.

[5] Sotoodeh M, Sozzi L, Vinay A, *et al.* Stepping toward standard methods of small-signal parameter extraction for HBT's[J]. *IEEE Trans. Microwave Theory Tech.*, 2000, **47**:1139 - 1151.

[6] Wei C J, Huang C M. Direct extraction of equivalent circuit parameters for heterojunction bipolar transistor[J]. *IEEE Trans. Microwave Theory Tech.*, 1995, **43**:2035 - 2039.

[7] Wang H, Ng G I, Zheng H, *et al.* Demonstration of aluminumfree metamorphic InP/In0.53Ga0.47As/ InP double heterojunction bipolar transistors on GaAs substrates[J]. *IEEE Electron Device Letter*, 2000, **21**(9):379 - 381.

[8] Yang H, Wang H, Radhakrishnan K. Thermal resistance of metamorphic InP-Based HBTs on GaAs substrates using a linearly graded InxGa1-xP metamorphic buffer[J]. *IEEE Trans. Electron Devices*, 2004, **51**(8):1221 - 1227.